

Generator Protection Overcomes Current Transformer Limitations

Marcos Donolo, Armando Guzmán, Mangapathirao V. Mynam,
Rishabh Jain, and Dale Finney
Schweitzer Engineering Laboratories, Inc.

Presented at the
41st Annual Western Protective Relay Conference
Spokane, Washington
October 14–16, 2014

Generator Protection Overcomes Current Transformer Limitations

Marcos Donolo, Armando Guzmán, Mangapathirao V. Mynam, Rishabh Jain, and Dale Finney,
Schweitzer Engineering Laboratories, Inc.

Abstract—Following industry standards to select current transformers (CTs) is the best way to avoid relay misoperations caused by CT saturation.

Differences in the saturation characteristics of CTs used in generator differential protection can lead to uneven CT saturation during external events, such as transformer energization, which may result in the undesired operation of generator differential elements.

In this paper, we review the challenges presented to generator differential protection elements in installations where a large spurious operating current appears during external events and examine adaptive protection elements that address these challenges.

I. INTRODUCTION

The IEEE Guide for the Application of Current Transformers Used for Protective Relaying Purposes recommends selecting identical current transformers (CTs) and burden impedances for differential relaying in generator protection applications [1]. For cases where identical CTs are not viable, the guide provides recommendations on how to match the CTs to avoid undesired differential element operations.

Differences in the saturation characteristics of the CTs lead to uneven CT saturation during external events, such as transformer energization, which may result in undesired operations of generator differential elements.

Typically, external events are the subject of interest for generator differential element security [2] [3] [4]. One such event, the black start procedure, requires that the generator energizes an unloaded transformer. This transformer energization generates significant unipolar inrush current that can cause uneven CT saturation and challenges the security of the differential elements.

The inherent design of a percentage differential element, which requires the operating current to be greater than a percentage of the restraining current to operate, tolerates some level of CT error caused by CT mismatch [5]. Modern differential elements used in busbar and transformer differential applications include logic to detect external events and switch the differential element to a high-security mode [6] [7]. Logic is also provided to revert the element back to a high-sensitivity mode when the conditions return to normal or upon detection of an internal fault.

This paper discusses a generator percentage differential element that uses external event detection logic to provide additional security for external events without sacrificing dependability.

II. CT SATURATION AND RECOMMENDATIONS FOR CT SELECTION

The equivalent circuit of a CT is shown in Fig. 1. The primary current reflected to the secondary winding is I_p/n . R'_p is the primary conductor resistance reflected to the secondary winding, and X'_p is the primary leakage reactance reflected to the secondary winding. R_s is the secondary conductor resistance and X_s is the secondary leakage reactance. The impedance $R_E||jX_M$ represents the magnetization branch. The excitation current I_E has two components: one that generates the flux in the CT core and one that represents the losses due to core hysteresis and eddy currents. The secondary excitation voltage E_s is the voltage induced in the secondary winding. The impedance Z_B represents the total load connected to the CT secondary winding, including the secondary cabling, the relay, and other connected loads. The CT secondary terminal voltage V_s appears across the CT burden.

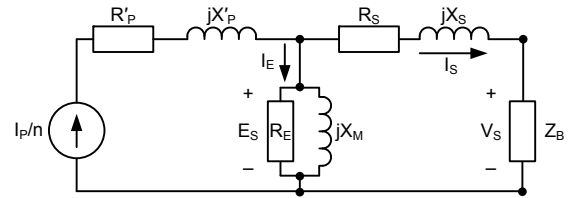


Fig. 1. CT equivalent circuit referred to the secondary side.

The relationship between excitation current and flux is linear for low values of excitation current. However, as flux levels increase, the core enters into saturation and the relationship between excitation current and flux is no longer linear. Fig. 2 shows an excitation curve for a C200 CT. In this figure, the excitation voltage and excitation current are E_s and I_E from Fig. 1.

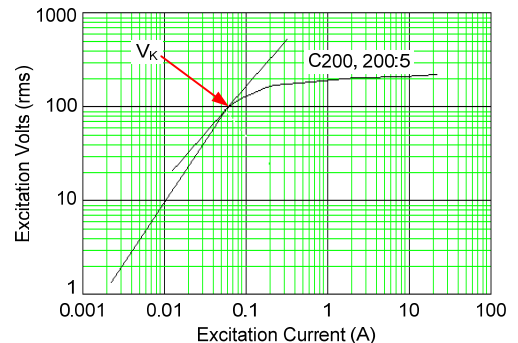


Fig. 2. Excitation characteristic of a C200 CT.

When V_S is low, the excitation current I_E is low and I_S is an almost perfect replica of I_P/n . As V_S increases due to an increase either of the primary current or the burden impedance, the excitation current increases. As E_S exceeds the knee-point voltage V_K in Fig. 2, a disproportionate amount of excitation current is required to produce further increases in flux. This increase in voltage drives the CT into saturation, and the secondary current is no longer a replica of the primary current.

A. Accuracy Class

CT accuracy can be expressed as a ratio error for relaying CTs. IEEE defines the ratio error as follows [1]:

$$\text{Ratio error (\%)} = \frac{I_E}{I_S} \cdot 100 \quad (1)$$

For relaying CTs, IEEE defines a limit of 10 percent for the ratio error for a steady state and a symmetrical (no dc offset) secondary current equal to 20 times the rated secondary current at the standard burden. The accuracy class for a relaying CT is designated by a letter followed by a secondary terminal voltage rating (for example, C100).

The secondary terminal voltage rating is the minimum voltage that the CT delivers to a standard burden at 20 times the rated secondary current without exceeding a 10 percent ratio error:

$$V_{STD} = 20 \cdot I_{SRATED} \cdot Z_{BSTD} \quad (2)$$

where:

V_{STD} is the secondary terminal voltage rating.

I_{SRATED} is the rated secondary current.

Z_{BSTD} is the standard burden.

The IEEE standard burdens are 1, 2, 4, and 8 ohms. For 5 A CTs, the standard secondary terminal voltage ratings are 100, 200, 400, and 800 V. For example, a C400 accuracy class on a 5 A CT means that the ratio error will not exceed 10 percent for any current from 1 to 20 times the rated current (5 to 100 A) or for any burden not exceeding the 4-ohm standard burden.

For Class C CTs, the ratio error will not exceed 10 percent if the secondary terminal voltage V_S is not greater than the secondary terminal voltage rating V_{STD} . AC saturation occurs when V_S exceeds V_{STD} as a result of symmetrical current.

B. CT Transient Operation

The previous section discussed CT performance in response to symmetrical currents. AC saturation can occur in a fraction of a cycle. However, fault and inrush currents frequently contain an exponentially decaying component (dc offset), which may produce significant CT saturation.

In general, the fault current in an inductive network takes the following form:

$$I_{FLT}(t) = I_{peak} \left[\sin(\omega t + \gamma - \theta) - e^{-\frac{R}{L}t} \sin(\gamma - \theta) \right] \quad (3)$$

where:

γ is the fault incident angle at $t = 0$.

θ is $\tan^{-1}\left(\frac{\omega L}{R}\right)$.

Saturation that occurs primarily as a result of the dc component is sometimes referred to as dc saturation. Equation (4) gives the criterion for saturation-free operation for a fault current that includes a dc offset [1] [8]:

$$20 \geq \left(\frac{X}{R} + 1\right) \cdot I_F \cdot Z_B \quad (4)$$

where:

I_F is the maximum fault current in per unit of the CT rating.

Z_B is the CT burden in per unit of the standard burden.

$\frac{X}{R}$ is the X/R ratio of the primary fault circuit.

Notice that this equation considers only a fully offset sinusoidal fault current and does not take into account inrush currents, which are not sinusoidal. The appendix in this paper provides information on how to model a CT.

The initial external fault contribution of a synchronous generator is limited by the subtransient reactance X_d'' , which has a value in the range of 0.1 to 0.15 per unit. This means that the initial fault current will be in the range of 6.67 to 10 per unit, and ac saturation will not be a big concern. However, for a synchronous generator, the primary system X/R ratio can be very large, often greater than 65. Additionally, during transformer energization, unipolar inrush currents contain a significant dc component. Consequently, dc saturation of CTs is a concern for generator relaying applications.

C. IEEE C37.110 Guidance for CT Selection

Generator differential protection has an advantage over other differential schemes (e.g., bus and transformer) in that there are always only two CTs forming the differential zone and these two CTs see approximately the same current during an external event. Section 7.2.2 of IEEE C37.110-2007 gives detailed guidance for the selection of CTs for generator differential protection [1]. Specifically, it states that CTs should be continuously rated to carry 120 to 150 percent of the

generator nominal current and should be selected with the highest secondary voltage rating (C class) that can be practically installed. The guide goes on to state: “The differential CTs on both sides of a generator should be of the same ratio, rating, connected burden, and preferably have the same manufacturer so that the excitation characteristics are well matched” [1].

The previous statement is intended to ensure that the two CTs forming the differential zone will saturate similarly, thereby minimizing the possibility of a spurious differential current. Note that matching the C class does not guarantee that the CT excitation characteristics will be the same.

The size of the switchgear limits the dimensions of the CT and the voltage rating a user can select. In addition, there can be significant differences in the lengths of the secondary cables. Finally, the two CTs may have been provided through different contracts (one for the generator and another for the switchgear). Under this circumstance, it is difficult to ensure that the CTs are built by the same manufacturer. In these installations, external events challenge the security of the differential elements.

III. BLACK STARTING

Black starting is the process of bringing the power system back to normal operation after a blackout without relying on power from an external transmission network. Regulatory bodies and utilities have restoration procedures to facilitate this process. The restoration procedures involve starting up generating units that are able to be started without power from an external transmission network. These units then energize the transmission lines and provide auxiliary power to start other generating units and ultimately restore service to the utility customers. For system restoration to be effective, the North American Electric Reliability Corporation (NERC) provides a group of standards that address black start emergency preparedness and operations [9]. Highlights of this standard include the following:

- Each transmission operator must have a documented black start resource testing procedure. Once every three years, this procedure must be tested on each black start generator.
- Field personnel must be provided with a minimum of two hours of system restoration training once every two years.
- Each transmission operator must have detailed plans of the restoration process and personnel prepared to enable effective coordination of the restoration process.

Any failure in the transmission system equipment, controls, or communications equipment jeopardizes the restoration process.

In some operating procedures, the black start generator is first brought up to its rated speed and voltage. The circuit breaker is then closed to energize the step-up transformer. This energization can generate significant unipolar inrush with a long time constant. This primary current has a significant dc component that can saturate the CTs fast and deep, providing

a challenge to the differential protection. In some scenarios, where the breaker between the generator and the step-up transformer is closed prior to starting the black start generator, the generator and transformer are energized together as the generator comes up to its rated voltage and speed and there are no inrush current problems.

Inrush and CT saturation phenomenon can also be experienced in industrial and commercial installations when backup generators are started following an outage at the facility.

Fig. 3 shows the currents captured from the CTs in the differential zone during a black start field test. Notice the unipolar inrush current through the CTs; the CTs start to saturate in the third cycle, as indicated by the offset in the flat portion of the currents. As the two CTs reach different levels of saturation, the two waveforms become more dissimilar. This dissimilarity leads to a spurious differential current that could potentially cause differential element operation.

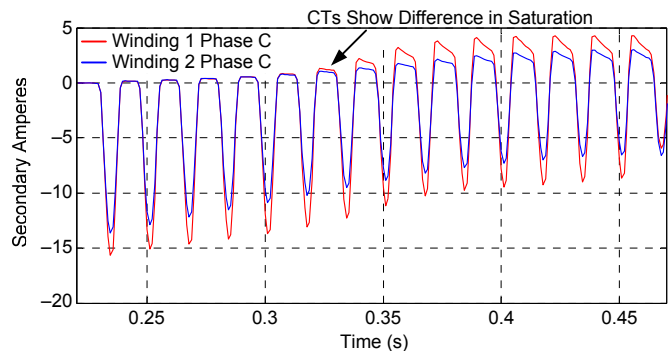


Fig. 3. Uneven CT saturation generates a spurious differential current.

IV. GENERATOR DIFFERENTIAL ELEMENT WITH EXTERNAL EVENT DETECTION LOGIC

A. Percentage Differential Element Principle

Differential protection operates on the sum of currents entering the protected zone. This sum, called differential or operating current, is proportional to the fault current for internal faults and approaches zero for any other operating condition.

In this paper, we consider protective relays that include three independent phase differential elements. Each differential element operates based on the phase currents of the terminal and neutral sides of the generator windings. Fig. 4 shows the current connections of one of these protective relays with the protected zones of each differential element shown with a red dotted line.

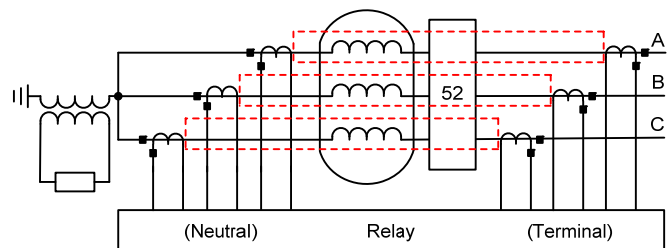


Fig. 4. Current measurements used by the generator differential element.

While an internal fault is the only condition leading to valid operating currents in the primary system, spurious operating currents in the secondary circuit result when the terminal- and neutral-side CTs respond differently for the same through current.

The sources of these spurious operating currents are CT and relay measurement errors. To address this issue, percentage differential elements define a restraining current proportional to the through current and assert its output if the operating current is greater than a minimum pickup threshold and also greater than a percentage of the restraining current:

$$(I_{OP} > O87PU) \text{ and } (I_{OP} > SLP \cdot I_{RT}) \quad (5)$$

where:

I_{OP} is the operating current.

I_{RT} is the restraining current.

O87PU is the minimum pickup threshold.

SLP is a scaling factor.

These two conditions determine the operating characteristic shown in Fig. 5.

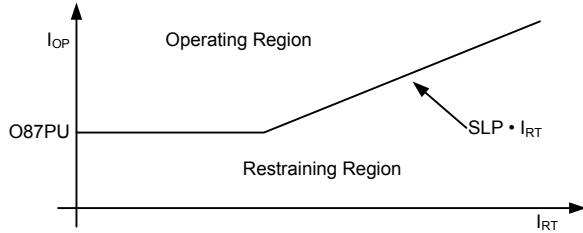


Fig. 5. Differential element operating characteristic.

B. External Event Detection Logic Improves Security Under CT Saturation Conditions

Large spurious operating currents result for external events when the CTs operate at different points on their corresponding excitation characteristics. Applying IEEE C37.110 minimizes these spurious operating currents by selecting appropriate CTs and burdens. When matching CTs is not practical, spurious differential currents resulting from external events, such as transformer energization, can cause undesired differential element operations. To minimize these undesired operations, modern digital protective relays include external event detection logic that provides additional security.

To avoid differential element operation for external events, the differential element switches to a high-security mode with a higher operating current pickup (O87PU2) and higher percentage slope (SLP2) when an external event is detected. Fig. 6 shows the sensitive characteristic and the high-security characteristic.

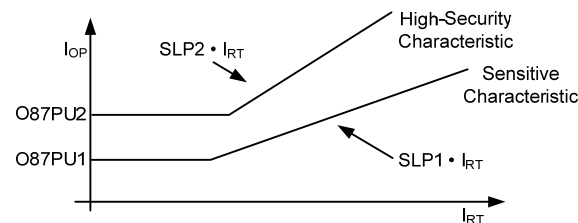


Fig. 6. Sensitive and high-security differential element characteristics.

The external event detection logic uses three principles of operation to control switching between the two characteristics.

1) Detecting External Faults Using the Operating and Restraining Currents

The first principle is that for external events, the relay initially detects change in the incremental restraining current and no change in the incremental operating current. When these conditions are detected for longer than the pickup delay of the timer shown in Fig. 7, the external event detection (EED) bit asserts. The relay uses this bit to activate the high-security mode of operation. This principle assumes that both CTs accurately reproduce the primary current for at least half a cycle.

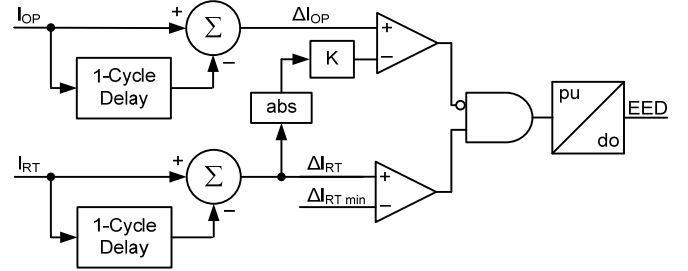


Fig. 7. A change in restraining current not accompanied by a change in operating current asserts the output of the external event detector.

2) Detecting External Events Using Current Distortion Information

The second principle is that external events and severe CT saturation cause, in many cases, harmonic distortion in the CT and secondary currents. The detection of this distortion can be used to extend the time that the differential element is in the high-security mode beyond the deassertion of EED.

Fig. 8 shows logic using the second harmonic to implement this principle. It is important to note that the second-harmonic restraint logic uses the terminal- and neutral-side currents rather than the operating current. Using terminal- and neutral-side currents makes the second-harmonic restraint logic sensitive to the detection of distortion in through currents. The logic includes a 5-cycle timer that allows tripping of the differential element for internal faults with second-harmonic distortion.

Comparator C1 in Fig. 8 asserts when the second-harmonic content in the Phase A terminal current ($IA1_2H$) exceeds a predefined threshold ($K2H = 0.1$ per unit), and Comparator C2 asserts when the second-harmonic content is larger than a fraction ($KF = 0.2$ per unit) of the fundamental current $IA1_F$ measured at the terminals of the generator. This same logic is used for the current measurement at the neutral side of Phase A and the terminal and neutral currents on Phases B and C. The relay uses the HRT bit to select the high-security characteristic of the differential element.

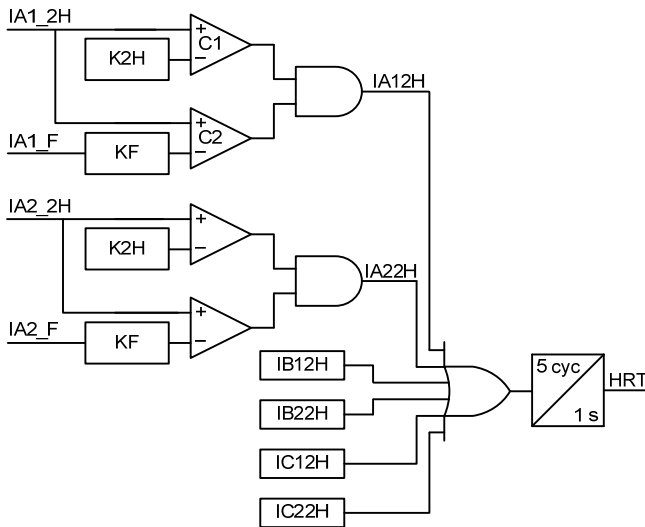


Fig. 8. Second-harmonic restraint logic.

3) Phase Comparator

The third principle is to switch the differential element back to the high-sensitivity mode if there is any indication that the external event has evolved into an internal fault. We use a current phase comparator to detect these evolving faults, as shown in Fig. 9. This comparator switches the element into the high-sensitivity mode when the angle difference between the terminal- and neutral-side currents is less than 90 degrees. The logic is supervised by a minimum restraining current value.

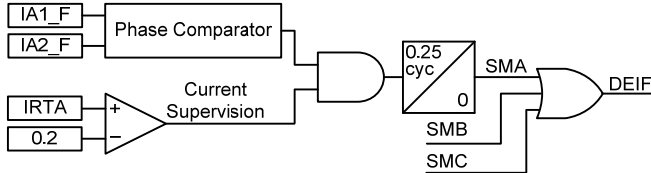


Fig. 9. Phase comparator logic.

The outputs of the logic shown in Fig. 7, Fig. 8, and Fig. 9 are then combined according to Fig. 10 to control the switching of the differential element to high-security mode (HSM).

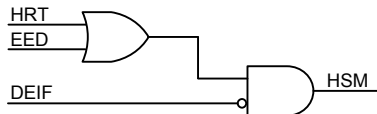


Fig. 10. Logic to activate the high-security mode in the differential element.

C. Performance of the Differential Element With the External Event Detector

In this section, we present Real Time Digital Simulator (RTDS[®]) simulation results to verify the performance of the differential element. We first show results for internal faults to verify that the external fault detection logic does not add delay to the operation of the differential element. We then verify

that the improved differential element does not operate for a transformer energization that would cause the traditional element to operate. Finally, we show the behavior of the logic when an internal fault occurs while energizing the transformer.

1) Test System

We modeled a 500 MVA synchronous generator connected to a 22/512 kV delta-wye step-up transformer rated at 600 MVA. The generator was grounded through a 1,000-ohm resistance. For this analysis, we recorded current measurements at the terminal and neutral sides of the generator winding and used the average of the magnitudes of these currents to compute the restraining quantities. We set O87PU1 to 0.3 per unit, SLP1 to 30 percent, O87PU2 to 1 per unit, and SLP2 to 100 percent.

2) Internal Faults

In this subsection, we show that for internal faults the external event detector does not add a delay to the operation of the differential element. With the generator operating at 50 percent load, we simulated phase-to-phase faults with different fault resistances. We compared two sets of terminal- and neutral-side CTs. The first set was a pair of C100 CTs with matched burdens (10 ohms), and the second set was a pair of C100 CTs with unmatched burdens (the burden of the terminal-side CT was 10 ohms and the neutral-side CT was 5 ohms). As expected, the external event detector operating on changes of I_{OP} and I_{RT} , remained deasserted for all of these cases. We used C100 class CTs with a high burden to show extreme cases of CT saturation.

For all of these internal faults, the differential element operated in less than 30 milliseconds, as shown in Fig. 11. As expected, none of the external event detectors asserted for any of these faults. Therefore, the operating times are the same with and without the high-security logic enabled. The slight increase in operating time for higher resistance faults is the result of a reduction in the operating current.

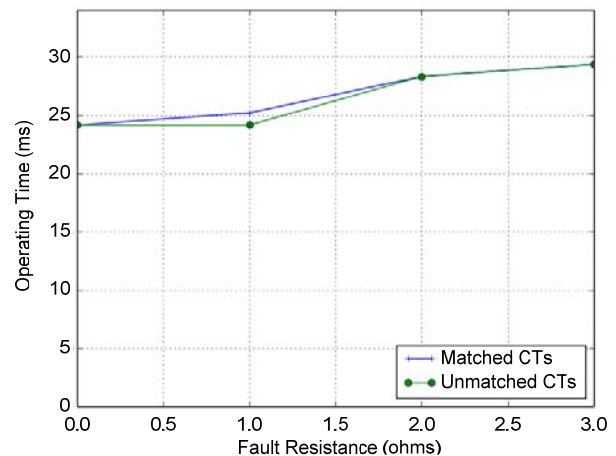


Fig. 11. Operating times for internal faults with fault resistance values of 0, 1, 2, and 3 ohms.

3) External Events

To show that the external event detector detects external events before the operation of the differential element, we consider the inrush current originated from energizing a transformer. We obtained CT secondary currents using three sets of C100 CTs. The first set consisted of a matched pair of CTs with a 10-ohm burden on each. The burdens on the second set of CTs were 5 and 10 ohms. On the third set of CTs, the burdens were 1 and 10 ohms. These extreme cases of burden mismatch were selected to demonstrate the effectiveness of the external event detection logic.

For these cases, the external fault detection logic asserted before the differential element, switched to the high-security mode, and avoided an undesired operation.

Fig. 12 through Fig. 15 show the Phase A terminal- (I_{A1}) and neutral-side (I_{A2}) secondary currents, the operating (I_{OP}) and restraining (I_{RT}) currents, and the response of the logic. EED is the output from the external event detector (Fig. 7), 87S is the output of a traditional differential element, and 87R is the response of a differential element with external event detection logic.

These figures show that all of the CT sets generated a large increment in the restraining current at the inception of the external event. Fig. 12 shows that the matched set of CTs did not generate any spurious operating current. The unmatched sets of CTs (Fig. 13 and Fig. 14) generated sufficient operating current to cause the traditional differential element (87S) to operate undesirably. The EED detected the external event and switched to the HSM, avoiding an undesired operation of the 87R.

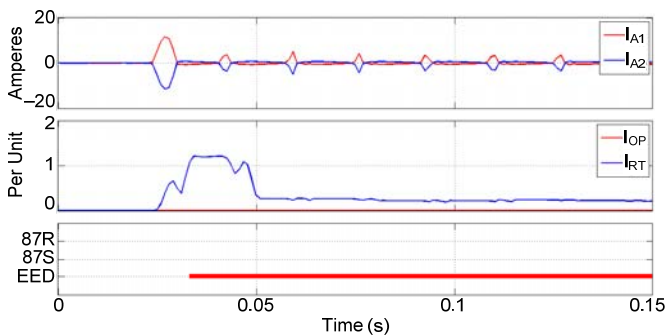


Fig. 12. Traditional and improved differential elements behave well with matched CTs. The burdens of the terminal- and neutral-side CTs are 10 ohms (all CTs are C100).

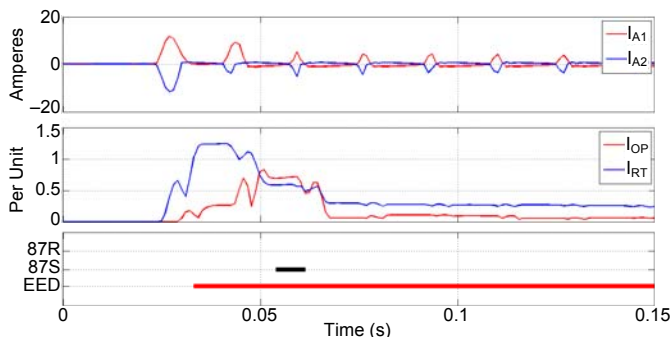


Fig. 13. The external event detector avoids misoperation with unmatched CTs. The burden of the terminal-side CT is 10 ohms and the neutral-side CT is 5 ohms (all CTs are C100).

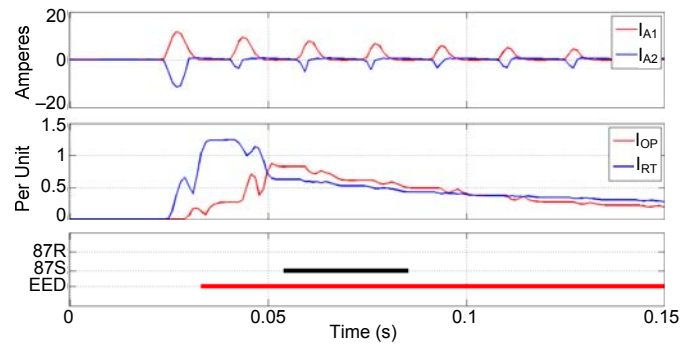


Fig. 14. The external event detection logic avoids misoperation even with extremely unmatched CTs. The burden of the terminal-side CT is 10 ohms and the neutral-side CT is 1 ohm (all CTs are C100).

While higher-class CTs provide increased security, burden mismatch can still cause undesired operations of the differential element.

To verify the performance when using higher class CTs, we replaced the C100 CTs with C200 CTs. The operating currents were reduced, but the reduction was not enough to avoid undesired operation of the traditional differential element, as shown in Fig. 15.

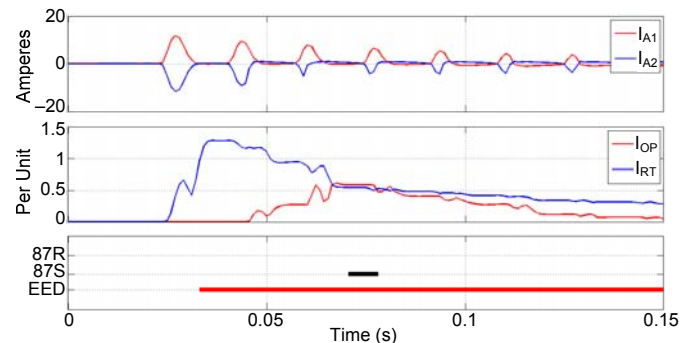


Fig. 15. Better CTs reduce operating current, but mismatched burdens can still cause traditional differential element operation for external disturbances. The burden of the terminal-side CT is 10 ohms and the neutral-side CT is 5 ohms (all CTs are C200).

4) Internal Fault During Transformer Energization

This subsection shows that the differential element with the external event detection logic has the sensitivity to detect internal faults even during external events. To test the performance, we considered an internal phase-to-phase fault 6 cycles after energizing the transformer.

The external event detection logic asserts during the transformer energization and forces the differential element into the HSM, avoiding an undesired operation. Fig. 16 shows the differential element operating times. The differential element operates while in the HSM for 0-, 1-, and 2-ohm fault resistances. For 3-ohm fault resistance, the differential element operates when the phase comparator (Fig. 9 and Fig. 10) switches the differential element back to its sensitive mode (Fig. 6).

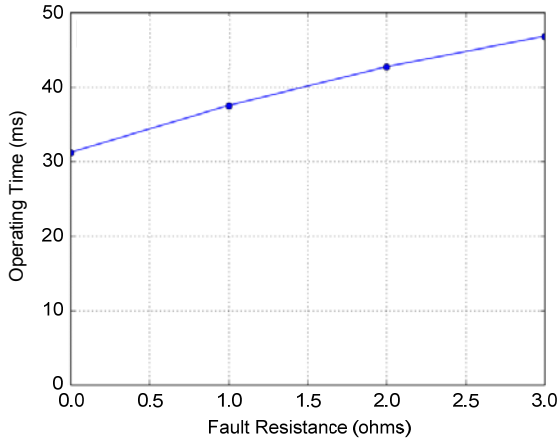


Fig. 16. Operating times for faults with different fault resistances occurring 6 cycles after transformer energization (the burden of the terminal-side CT is 10 ohms, the neutral-side CT is 5 ohms, and the CTs are C100).

V. PERFORMANCE OF OVERCURRENT ELEMENTS UNDER CT SATURATION CONDITIONS

Overcurrent elements operating on Fourier or cosine filters underreach during heavy CT saturation conditions. Fig. 17 shows the ratio current of one of the faulted phases for a phase-to-phase fault, the corresponding secondary current, and the magnitude of the output signal of a fundamental-frequency cosine filter [10]. Due to CT saturation, the magnitude of the cosine filter output signal is approximately 30 percent below the expected peak value.

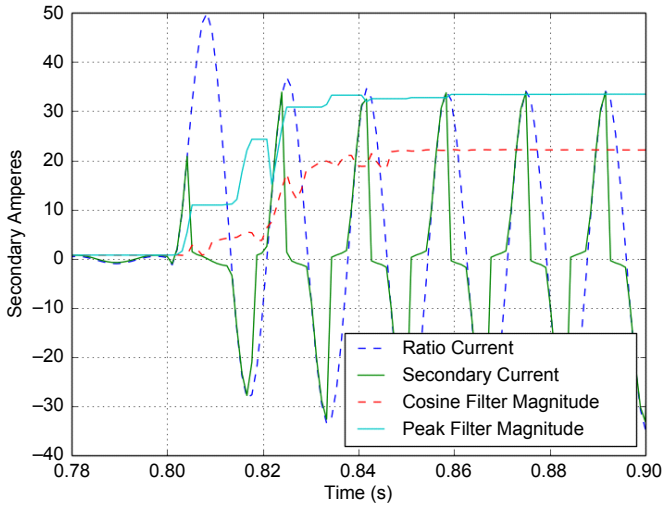


Fig. 17. Cosine filter performance under heavy CT saturation conditions.

Some protective relays include a cosine-peak adaptive filter to address the underreach limitation of overcurrent elements. This filter, as explained by Benmouyal and Zocholl in [11], uses the peak detector filter output whenever the relay detects CT saturation.

The output of the peak detector filter consists of the average of the absolute value of the maximum and minimum samples within the latest cycle. Fig. 17 shows the magnitude of the peak detector output. Note that after 3 cycles the output of the peak detector filter closely matches the magnitude of the ratio current.

VI. CONCLUSION

In this paper, we present an adaptive generator differential element with two characteristics. Under normal conditions, the element operates with a sensitive characteristic. Upon the detection of external events, the element operates with a high-security characteristic to avoid undesired operations.

To detect external events, the adaptive differential element uses incremental operating and restraining quantities and the second-harmonic content of winding currents. A phase comparator detects internal fault conditions during external events and switches to the sensitive characteristic for the differential element to operate.

Overall, following the IEEE C37.110 guidelines to select CTs and using the proposed logic minimize the risk of undesired relay operation caused by CT saturation.

VII. APPENDIX: CT MODEL

CT modeling plays a key role in analyzing the performance of protective relays and differential elements in particular. Fig. 18 shows the classical circuit used to model a CT.

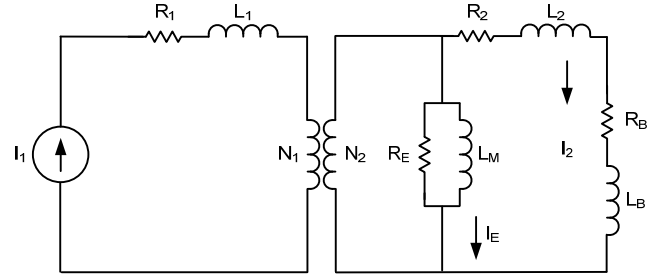


Fig. 18. CT equivalent circuit.

In Fig. 18:

N_1 is the number of turns in the primary winding.

N_2 is the number of turns in the secondary winding.

I_1 is the primary current in amperes.

I_2 is the secondary current in amperes.

I_E is the excitation current in amperes.

R_1 is the resistance of the primary winding in ohms.

L_1 is the inductance of the primary winding in henries.

R_2 is the resistance of the secondary winding in ohms.

L_2 is the inductance of the secondary winding in henries.

R_E is the resistance of the magnetizing branch in ohms.

L_M is the inductance of the magnetizing branch in henries.

R_B is the burden resistance in ohms.

L_B is the burden inductance in henries.

The circuit in Fig. 18 can be simplified, as shown in Fig. 19. The simplified circuit shows the primary ratio current, $(N_1/N_2) \cdot I_1$, the current in the magnetizing branch I_M , and the secondary current I_2 . The simplified circuit neglects the R_1 and L_1 components of the primary winding and the losses represented by R_E in the magnetization branch. This circuit includes the R_B and L_B components in the corresponding R_2 and L_2 components.

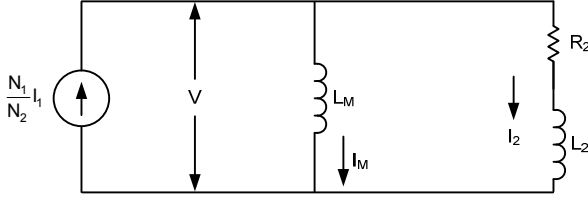


Fig. 19. Simplified CT equivalent circuit to model CT saturation.

The voltage across the magnetization branch is the same as the voltage across the equivalent secondary branch. Using Faraday's law and Kirchoff's voltage law, we express this voltage, which is proportional to the derivative of the magnetic flux ϕ (in Wb) with respect to time, according to (6) and (7).

$$V = N_2 \frac{d\phi}{dt} = L_M \frac{dI_M}{dt} \quad (6)$$

$$V = N_2 \frac{d\phi}{dt} = I_2 R_2 + L_2 \frac{dI_2}{dt} \quad (7)$$

L_M is proportional to the permeability μ (in H/m), the cross area of the CT core A (in m^2), and the length of the magnetic flux path inside the CT core ℓ (in m). N_2^2 is the proportionality constant, as shown in (8).

$$L_M = N_2^2 \cdot \frac{\mu A}{\ell} \quad (8)$$

We represent the voltage V as a function of the magnetic flux densities B and A , I_M in terms of the primary ratio current, and I_2 , according to (9) and (10).

$$V = N_2 A \frac{dB}{dt} = L_M \left(\frac{N_1}{N_2} \frac{dI_1}{dt} - \frac{dI_2}{dt} \right) \quad (9)$$

$$V = N_2 A \frac{dB}{dt} = I_2 R_2 + L_2 \frac{dI_2}{dt} \quad (10)$$

We use the empirical Frölich equation to determine μ from $B = 0$ to $B = B_{SAT}$, as shown in (11), and use $\mu = \mu_0$ for $B > B_{SAT}$ [12].

$$\mu = \left(1 - \frac{1 - \frac{1}{\sqrt{\mu_{Ri}}}}{B_{SAT}} |B| \right)^2 \mu_{Ri} \mu_0 \quad (11)$$

where:

μ_{Ri} is the initial permeability.

μ_0 is the free space permeability (H/m).

B_{SAT} is the saturation magnetic flux density (T).

We solve (9) and (10) to obtain the derivatives of the flux density B and the secondary current I_2 with respect to time, according to (12) and (13).

$$\frac{dB}{dt} = \frac{\mu \left(N_1 L_2 \frac{dI_1}{dt} + N_2 R_2 I_2 \right)}{\ell L_2 + N_2^2 \mu A} \quad (12)$$

$$\frac{dI_2}{dt} = \frac{N_1 N_2 \mu A \frac{dI_1}{dt} - \ell R_2 I_2}{\ell L_2 + N_2^2 \mu A} \quad (13)$$

The area of the CT core can be approximated using the class of the CT V_{STD} (in V), the saturation flux density B_{SAT} , and the number of turns of the secondary winding N_2 , according to (14).

$$A = \frac{V_{STD}}{\omega N_2 B_{SAT}} \quad (14)$$

where:

ω is the power system frequency (rad/s).

We use (15) and the power system shown in Fig. 20 to obtain the primary current as a function of time, $I_1(t)$, where R_{SYS} and L_{SYS} are the equivalent power system resistance and inductance.

$$I_1(t) = \sqrt{2} I_{RMS} \left[\sin(\omega t + \gamma - \theta) - e^{-\frac{R_{SYS} t}{L_{SYS}}} \sin(\gamma - \theta) \right] \quad (15)$$

where:

γ is the fault incident angle at $t = 0$.

θ is $\tan^{-1} \left(\frac{\omega L_{SYS}}{R_{SYS}} \right)$.

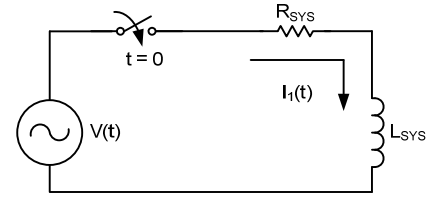


Fig. 20. Basic R-L circuit to calculate the primary current.

VIII. REFERENCES

- [1] IEEE Standard C37.110-2007, IEEE Guide for the Application of Current Transformers Used for Protective Relaying Purposes.
- [2] S. E. Zocholl, "Standard CT Accuracy Ratings in Metal-Clad Switchgear," proceedings of the 59th Annual Conference for Protective Relay Engineers, College Station, TX, April 2006.
- [3] H. J. Altuve, N. Fischer, G. Benmouyal, and D. Finney, "Sizing Current Transformers for Line Protection Applications," proceedings of the 66th Annual Conference for Protective Relay Engineers, College Station, TX, April 2013.
- [4] B. Kasztenny and D. Finney, "Generator Protection and CT Saturation Problems and Solutions," proceedings of the 58th Annual Conference for Protective Relay Engineers, College Station, TX, April 2005.
- [5] R. E. Cordray, "Percentage-Differential Transformer Protection," *Electrical Engineering*, Vol. 50, Issue 5, May 1931, pp. 361–363.
- [6] A. Guzmán, B. Qin, and C. Labuschagne, "Reliable Busbar Protection With Advanced Zone Selection," *IEEE Transactions on Power Delivery*, Vol. 20, Issue 2, April 2005, pp. 625–629.
- [7] A. Guzmán, N. Fischer, and C. Labuschagne, "Improvements in Transformer Protection and Control," proceedings of the 62nd Annual Conference for Protective Relay Engineers, College Station, TX, March 2009.
- [8] S. E. Zocholl, *Analyzing and Applying Current Transformers*. Schweitzer Engineering Laboratories, Inc., Pullman, WA, 2004.
- [9] NERC Standard EOP-005-2 – System Restoration from Blackstart Resources. Available: <http://www.nerc.com>.
- [10] E. O. Schweitzer, III, and D. Hou, "Filtering for Protective Relays," proceedings of the 19th Annual Western Protective Relay Conference, Spokane, WA, October 1992.

- [11] G. Benmouyal and S. E. Zocholl, "The Impact of High Fault Current and CT Rating Limits on Overcurrent Protection," proceedings of the 29th Annual Western Protective Relay Conference, Spokane, WA, April 2002.
- [12] R. Garret, W. C. Kotheimer, and S. E. Zocholl, "Computer Simulation of Current Transformers and Relays for Performance Analysis," proceedings of the 14th Annual Western Protective Relay Conference, Spokane, WA, October 1987.

IX. BIOGRAPHIES

Marcos Donolo received his BSEE from Universidad Nacional de Río Cuarto, Argentina, in 2000 and his master's degree in electrical engineering (2002), his master's degree in mathematics (2005), and his Ph.D. in electrical engineering (2006) from the Virginia Polytechnic Institute and State University. Since 2006, he has been with Schweitzer Engineering Laboratories, Inc., where he is presently a lead research engineer. He holds several patents and has authored numerous papers related to power system protection. He is a senior member of IEEE.

Armando Guzmán received his BSEE with honors from Guadalajara Autonomous University (UAG), Mexico. He received a diploma in fiber-optics engineering from Monterrey Institute of Technology and Advanced Studies (ITESM), Mexico, and his MSEE and MECE from the University of Idaho, USA. He lectured at UAG and the University of Idaho on power system protection and power system stability. Since 1993, he has been with Schweitzer Engineering Laboratories, Inc. in Pullman, Washington, where he is a fellow research engineer. He holds numerous patents in power system protection and metering. He is a senior member of IEEE.

Mangathirao (Venkat) Mynam received his MSEE from the University of Idaho in 2003 and his BE in electrical and electronics engineering from Andhra University College of Engineering, India, in 2000. He joined Schweitzer Engineering Laboratories, Inc. (SEL) in 2003 as an associate protection engineer in the engineering services division. He is presently working as a senior research engineer in SEL research and development. He was selected to participate in the U.S. National Academy of Engineering (NAE) 15th Annual U.S. Frontiers of Engineering Symposium. He is a senior member of IEEE.

Rishabh Jain received his B.Tech. in electrical engineering from the Indian School of Mines, India, and his MS from the University of Idaho, U.S., in 2011 and 2014, respectively. He worked as a research engineering intern in the Power Systems Research group at Schweitzer Engineering Laboratories, Inc. until July 2014. Currently, he is pursuing his Ph.D. from North Carolina State University and works at the FREEDM Systems Center. His research interests are in the grid integration of distributed generation, microgrid applications, power system protection, and converter designs.

Dale Finney received his BSEE from Lakehead University and his MSEE from the University of Toronto. He began his career with Ontario Hydro, where he worked as a protection and control engineer. Currently, he is employed as a senior power engineer with Schweitzer Engineering Laboratories, Inc. His areas of interest include generator protection, line protection, and substation automation. He holds several patents and has authored more than 20 papers in the area of power system protection. He is a member of the main committee of the IEEE PSRC, a member of the rotating machinery subcommittee, and a registered professional engineer in the province of Nova Scotia.